Revista Brasileira de Ciência do Solo

Sediment source and volume of soil erosion in a gully system using UAV photogrammetry

Bernardo Moreira Cândido[(1)*] (iD)**, Mike James**[(2)] (iD)**, John Quinton**[(2)] (iD)**, Wellington de Lima**[(3)] (iD) **and Marx Leandro Naves Silva**[(3)] (iD)

[(1)] Instituto Agronômico de Campinas, Centro de Solos e Recursos Ambientais, Campinas, São Paulo, Brasil.
[(2)] Lancaster University, Lancaster Environment Centre, Lancaster, Lancashire, United Kingdom.
[(3)] Universidade Federal de Lavras, Departamento de Ciência do Solo, Lavras, Minas Gerais, Brasil.

* Corresponding author:
E-mail: b.candido@iac.sp.gov.br

ABSTRACT: Gully erosion is a severe way of land degradation. Gullies threaten the sustainability of agro-ecosystems, causing quantitative and qualitative reduction of groundwater, farmland productivity, and waterways sedimentation. Since the gully development on the surface begins with water flow and sheet erosion, accurate monitoring of the erosive processes in a gully system and its quantification is key for the development of effective strategies to control soil erosion in gullies. Here, we demonstrate the first use of unmanned aerial vehicle (UAV) and structure-from-motion/multiview-stereo photogrammetry to evaluate the relative contribution of the different types of erosion (sheet, rill, and gully sidewall) in the gully development. A gully located at Lavras, Brazil, was surveyed using a UAV equipped with a RGB camera. The Precision Maps (PM) variant of the Multiscale Model to Model Cloud Compare (M3C2) algorithm was used to calculate spatial changes in the soil surface topography and to quantify the volumes of sediments lost and gained in the gully system. The point clouds showed root mean square errors of order ~ 3 mm on *xyz* on check points. The spatial variation of precision along the gully ranged from 0.006 to 0.276 m, considering the M3C2-PM uncertainty values. The results revealed that the main source of sediment in the gully studied was due to the mass movement processes. Rills and laminar erosions contributed 8 and 3 %, respectively, to the total sediment yield, while the mass movements corresponded with most of the sediment generation in the gully. Of the total sediment produced in the system, only 24 % was stored in the gully, indicating its high activity and instability. For the first time, the sediment sources of a gully were quantified remotely and with millimetric precision. The UAV photogrammetry generated high-resolution measurements, allowing evaluation of the contribution of sheet erosion in the generation of sediment of the gully. This opens up new possibilities in the studies involving the dynamics of gullies, since the understanding of the spatial and temporal behaviour of the erosive processes are important in the development of control strategies and monitoring of the evolution of a gullies complex.

Keywords: sheet erosion, rill erosion, gully sidewall, structure-from-motion, precision maps.

INTRODUCTION

Gullies represent a significant source of sediments, especially in tropical environments (Poesen, 2011), reaching areas of about 3.5 ha for a single gully (Lin et al., 2015). Gully erosion can be defined as being an erosive process where the water concentrates in the landscape, being affected by the presence of tracks and the lack of conservation measurements in the area (Poesen et al., 2002; Valentin et al., 2005; Lin et al., 2015). The concentrated flow reduces topsoil by the gully initiation, causing severe impacts in farmland productivity and waterways sedimentation (Allen et al., 2018; Bastola et al., 2018; Zabihi et al., 2019).

Long-term studies report that gullies develop randomly and are linked with the natural mass movements associated with the removal of vegetation cover (Harvey, 1997; Lin et al., 2015). However, gully development involves several sub-processes related to water erosion and mass movements, such as detachment, transport, and deposition of sediments, gully bank retreat, piping and fluting (Harvey, 1992). The complex interaction between these sub-processes, with erosion and deposition occurring simultaneously in the area (Gómez-Gutiérrez et al., 2012), coupled with the three-dimensional nature of the gullies, make it difficult to measure and quantify directly in the field (De Rose et al., 1998; Poesen et al., 2003).

Traditional methods such as pins (Desir and Marín, 2007), microtopographic profiles (Casalí et al., 2006), surveys with total stations (Ehiorobo and Audu, 2012) and poles are being replaced by techniques based on high-resolution photogrammetry (Castillo et al., 2012). Several studies have quantified gully erosion through photogrammetry associated with three-dimensional soil surface reconstruction methods, such as structure-from-motion/multiview-stereo (SfM-MVS) (Castillo et al., 2012; Gómez-Gutiérrez et al., 2014; Kaiser et al., 2014; Di Stefano et al., 2017; Ben Slimane et al., 2018; Siqueira Junior et al., 2019).

Through SfM-MVS photogrammetry, it is possible to elucidate better the erosive processes that occur in the gully system, by obtaining digital elevation model (DEM) with high spatial and temporal resolution. With recent advances in the use and availability of unmanned aerial vehicles (UAV), the use of SfM-MVS photogrammetry to produce high-resolution DEM has become popular in geosciences (d'Oleire-Oltmanns et al., 2012; Carollo et al., 2015; Di Stefano et al., 2017), because it is cheap, less time-consuming, requires little knowledge due to the automation of processes, and has similar accuracy to the most accurate methods currently available, such as laser scanning (Castillo et al., 2012; James and Robson, 2012; Fonstad et al., 2013).

The knowledge of the contribution rates of rills and gully sidewalls and the quantification of sediments stored in the channels and lost from the gully system are important for the development of effective strategies to control soil erosion in gullies (Hosseinalizadeh et al., 2019). This spatial and temporal variation of sediments in gully development are indicators used by land managers to identify the stage of development and stabilization of the gully system (Betts et al., 2003). When the amount of lost sediment becomes smaller than that stored in the channels, it indicates a stabilization of the erosive process in the gully (Kasai et al., 2001).

Although many studies have described the formation and development processes of gullies (Harvey, 1992; Vandekerckhove et al., 1998; Sidorchuk et al., 2003; Conoscenti et al., 2014), few papers used the UAV photogrammetry for detailed study of sediment sources and their movement over time in the gully environment. Considering that gullies have a complex growth dynamic, the study of spatial and temporal evolution through high-resolution DEMs are important for the development of control strategies to mitigate sediment delivery in watercourses and soil erosion in degraded areas.

Changes in macro and microtopography of gully systems require the understanding of the continuous process of source-transport-deposition of sediments (Valentin et al., 2005). The objectives of this study were to use UAV photogrammetry to (1) determine the relative contribution of rills and gully sidewalls to sediment generation; (2) quantify the sediment volumes stored in channels and lost from the gully; and (3) quantify the total volume of sediments produced by the gully.

MATERIALS AND METHODS

Study area

The studied gully is located in a degraded area (Figure 1) on the *campus* of the Federal University of Lavras, Southeastern Brazil (21° 13' 37.3" S and 44° 59' 11.9" W). The study area has a humid subtropical climate classified as Cwa according to the Köppen Climate Classification System and an average annual rainfall of 1,530 mm. The gully has a total catchment area of 530 m^2.

Image acquisition for SfM-MVS

Images were acquired using the UAV DJI Phantom 3 Professional integrated with a gimbal-stabilized FC300X camera with 12-megapixel (4000 × 3000) Sony EXMOR 1/2.3 sensor, 94° field of view (FOV) and 20-mm focal length. The lens aperture was set to f/2.8 and images acquired in RAW format. Two flights were performed in the gully area, the first in October 2017 and the second in May 2018.

To cover the complex three-dimensional (3D) area of the gully, it was acquired oblique images, which also added to the strength of the network geometry (James et al., 2017a). However, as a result of the multiple camera angles, the overlap percentage between the images was highly variable (Figure 2a). Thus, the number of images in which some point is present was used as the metric to describe the image overlap. In this study, most areas were captured by more than 30 overlapping images because of the oblique angles. Surveys comprised about 300 images, which reflects the complex nature of the gully morphology. The flying height ranged between 5 and 15 m, resulting in a nominal ground sampling distance between 2 and 6 mm.

To compare the SfM-MVS results at different times, both surveys must be in the same coordinate system. Thus, for the georeferencing, 15 permanent ground control points
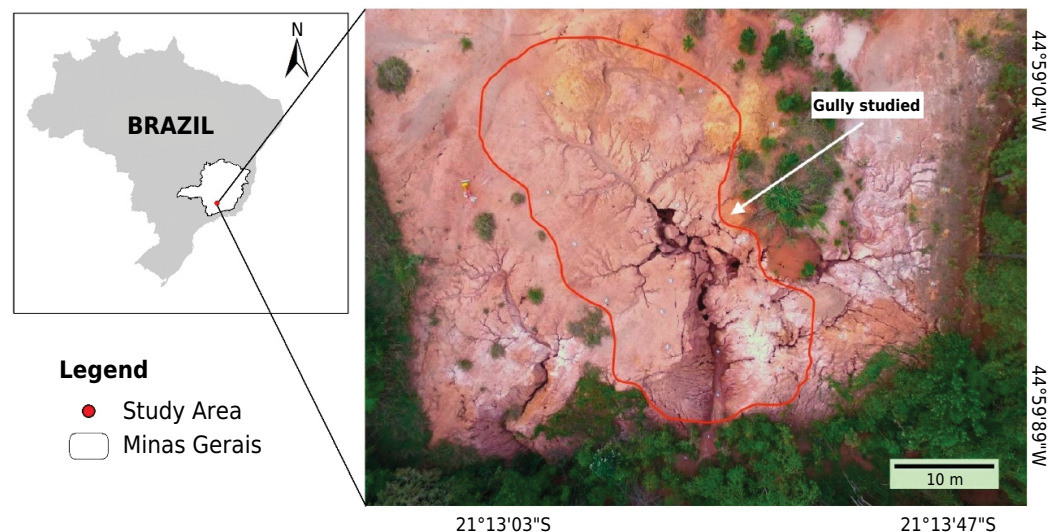
Figure 1. Location of the study area.

(GCP) were installed in the area (Figure 2b), with ten points used for control and five as check points to estimate the accuracy of the point clouds by calculating the root mean square error (RMSE). The GCP coordinates were determined by a total station (Geodetic GD2i, accuracy 2 mm), within an arbitrary local coordinate system.

SfM-MVS point cloud generation

The 3D point clouds were generated using the SfM-MVS photogrammetry technique, which allows the reconstruction of the topography from randomly distributed and oriented images from uncalibrated cameras (James and Robson, 2012; Fonstad et al., 2013). The sets of photographs were processed using the SfM-MVS commercial software Agisoft Photoscan v1.4.5. The photogrammetric errors were calculated by the Photoscan on x, y, and z-axes for the control, check and tie points of each SfM-MVS point cloud. The photogrammetric parameters used in Photoscan are listed in table 1. All surface reconstructions were done through cloud computing using a virtual machine with 24 cores, 128 GB RAM and two NVIDIA Tesla K80 GPUs.

Change detection and 3D precision maps

The soil surface changes between the different surveys were evaluated using the precision maps (PM) variant of the Multiscale Model to Model Cloud Compare algorithm
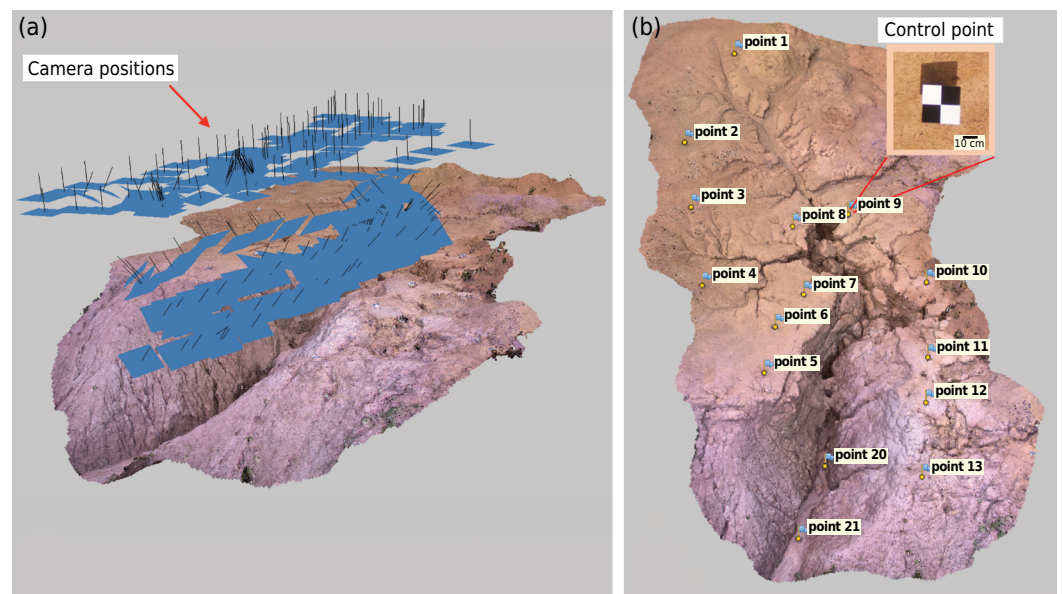
Figure 2. Annotated computer screenshot of Photoscan showing camera positions and orientations (a), and control point layout (b).

Table 1. Photoscan parameters settings used during the point cloud generation

Point cloud: alignment parameters	Setting
Accuracy	Highest
Generic preselection	Yes
Reference preselection	Yes
Key point limit	120,000
Tie point limit	0
Filter point by mask	No
Dense point cloud: reconstruction parameters	
Quality	High
Depth filtering	Mild

(M3C2; Lague et al., 2013), an analytical tool implemented in CloudCompare software. The M3C2-based approach is more appropriate for detecting change in complex 3D environments than DEM of Difference (DoD) (Lague et al., 2013). Comparisons using DEM can overestimate errors on steep terrain since small lateral shifts can produce large vertical differences (Cook, 2017).

The M3C2-PM algorithm finds the most appropriate normal direction for each point and calculates the distance between the two point clouds along a cylinder of a given radius projected along the normal. The comparisons used core points with 1 cm spacing, a cylinder with a 30 cm diameter, and multiscale normals with radii from 0.2 m to 1 m with a step of 0.2 m.

The native M3C2 uses a roughness-based metric to estimate precision, but this is not appropriate for photogrammetric point clouds (James et al., 2017b). Thus, in this study, maps of photogrammetric precision were used to obtain the confidence intervals in the detection of changes between the surveys. The M3C2-PM approach has a greater capacity to detect changes in areas of complex topography, such as gullies, considering the spatial and 3D variation of survey accuracy (James et al., 2017b). A detailed explanation of M3C2-PM is given by James et al. (2017b).

In this study, the precision estimates were derived by reprocessing the Photoscan using DBAT bundle adjustment (Murtiyoso et al., 2018), integrated into SfM_georef (James and Robson, 2012). The precision maps were generated through the interpolation (5-mm grid size) of the standard deviation derived by the precision estimates. It was used median as interpolation method to minimise the influence of outliers (James et al., 2017b).

To calculate the gully erosion volume, as well as the relative contribution of rill erosion and mass movements, the dense point clouds were interpolated (5-mm grid size) using the Kriging method. The zones related to each type of erosion were delimited considering as rills channels with more than 0.01 m in width and depth (Foster, 2005) and as gullies channels of at least 0.3 m in width and depth (Blanco and Lal, 2010). The volumes of sediments stored and lost from the gully system were calculated using the Simpson's rule method (Easa, 1988), which assumed non-linearity in the profile between the grid points. The volume calculations and maps were performed using Surfer16 software.

RESULTS

Accuracy of SfM-MVS point clouds

Both surveys had similar magnitudes of photogrammetric error (Table 2). The surveys showed RMSE of order ~ 3 mm on *xyz* on control and check points, whereas the tie point image residual root mean square (RMS) was ~ 0.6 pixels (Figure 3).

The precision maps show the spatial variation of precision on each survey along the gully, with M3C2-PM uncertainty values ranging from 0.006 to 0.276 m (Figure 4). The highest values were concentrated in shaded areas and at the bottom of the gully. Because of that, the first survey was less accurate than the second one, especially in the more complex areas.

Table 2. Photogrammetric errors of check points, control points and tie points image residuals

Date	Number of images	Dense cloud points	RMS tie points image residuals (pixel)	RMSE of control points (mm)			RMSE of check points (mm)		
				X	Y	Z	X	Y	Z
27/10/17	277	51,002,599	0.568	4.2	2.5	1.3	4.2	4.5	2.0
26/05/18	325	65,475,214	0.561	2.8	3.3	4.5	3.2	3.5	2.6

RMS: root mean square; RMSE: root mean square error.
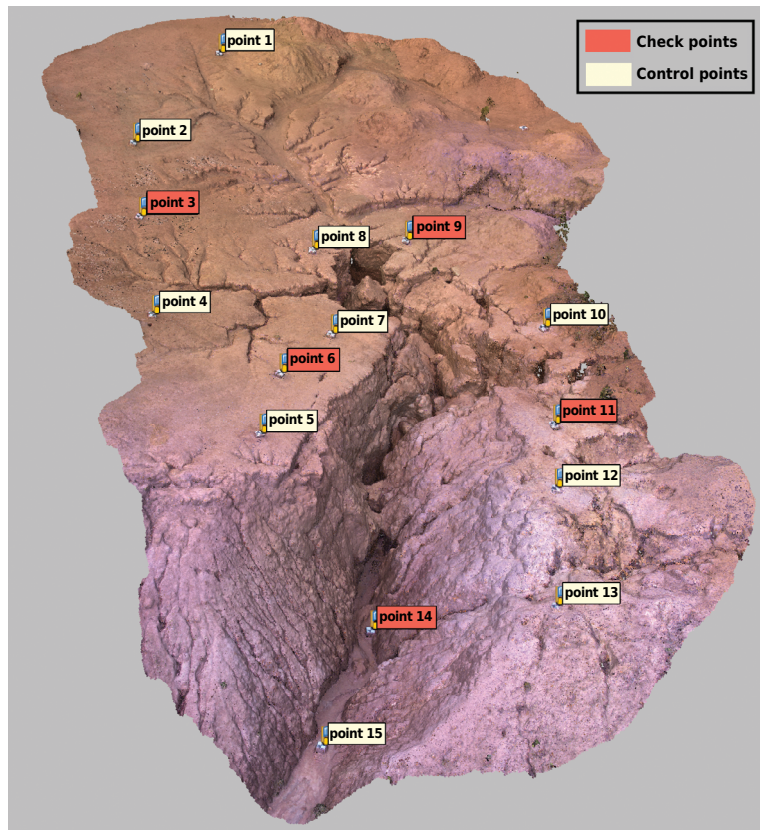
Figure 3. Location of the control and check points in the study area.
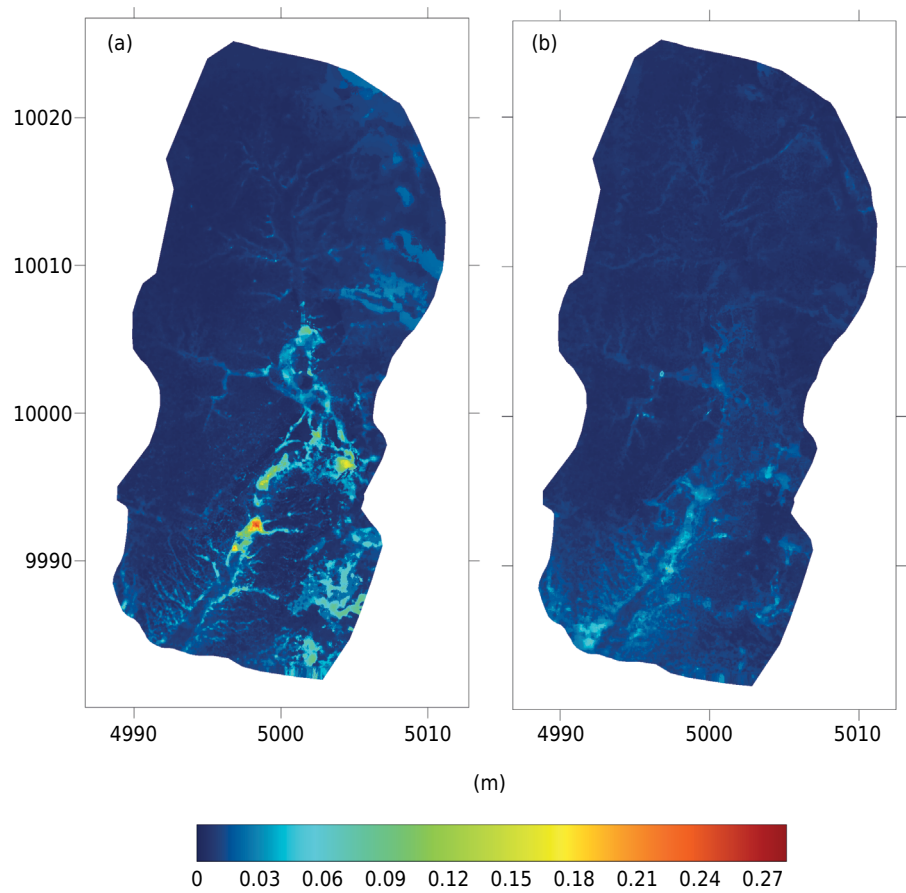
Figure 4. Precision maps showing the spatial variation of the error for both October 2017 (a) and May 2018 (b) surveys.

The image overlap, as well as the number of images, were sufficient to produce results with consistently good coverage. For gully erosion studies, gaps in coverage of only about 10-cm spacing can be problematic. The 3D reconstruction of the topography of the most complex areas of the gully was done adequately, reproducing with fidelity the terrain morphology (Figure 5).

Sediment source dynamics

The significant changes found by the M3C2-PM method showed a high visual correlation with the observed differences between both DEM in the area (Figure 6). Significant changes were detected in the topsoil, rill erosion, and in the mass movements, such as gully sidewalls, inside the gully.

During the study period, a total of 71 m^3 of sediments were generated (Table 3), and 76 % of this volume was lost from the gully system. Almost all sheet erosion was stored in the area, contributing with less than 1 % to the output of sediments from the gully. Rill erosion contributed 8 % of the sediment yield in the gully, in large part being lost in the erosion process and only 0.76 m^3 stored in the channels.

The mass movements, including gully sidewall erosion, corresponded to 89 % of the total sediments produced. However, 23 % of that volume was deposited and stored in the gully bed. Nevertheless, of the total soil loss from the system, more than 90 % was originated from the mass displacements promoted by the gully sidewall, while rill erosion accounted for approximately 9 % of the sediment lost. The dynamics of the gully development, as well as the contribution of gully side wall retreat, are well represented by the difference between the two point clouds obtained by M3C2-PM (Figure 7).

DISCUSSION

SfM-MVS measurements errors

For the study of active and dynamic environments, such as gullies, where the variations in the soil surface are in the order of centimetres and metres, RMSE values in the order of
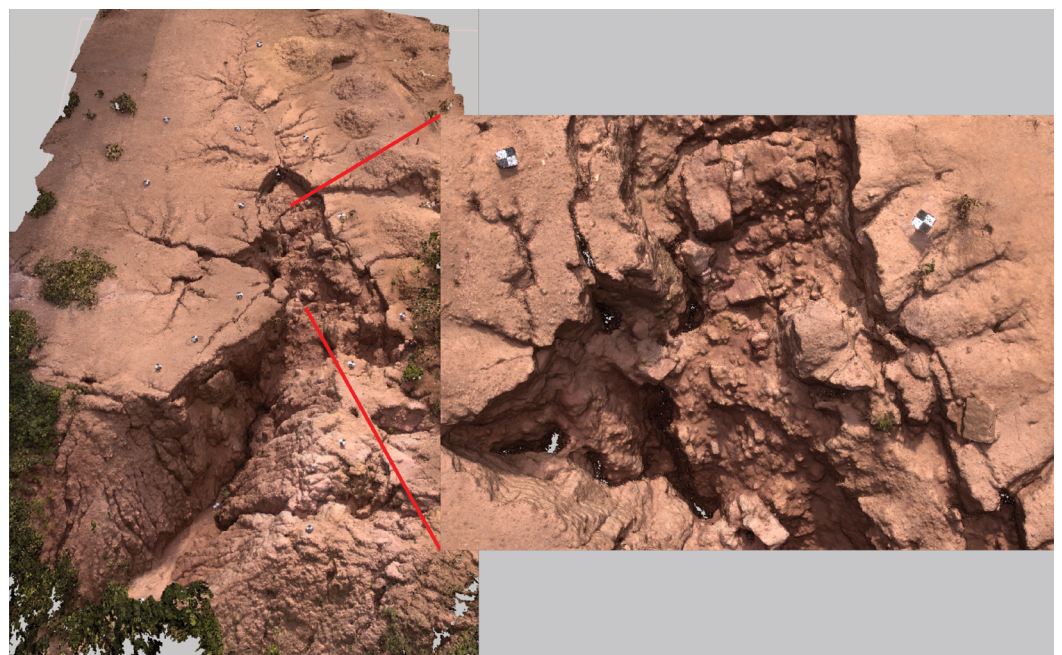
Figure 5. Dense point cloud showing the 3D reconstruction of complex topographic areas inside the gully.

27-10-2017   **26-05-2018**
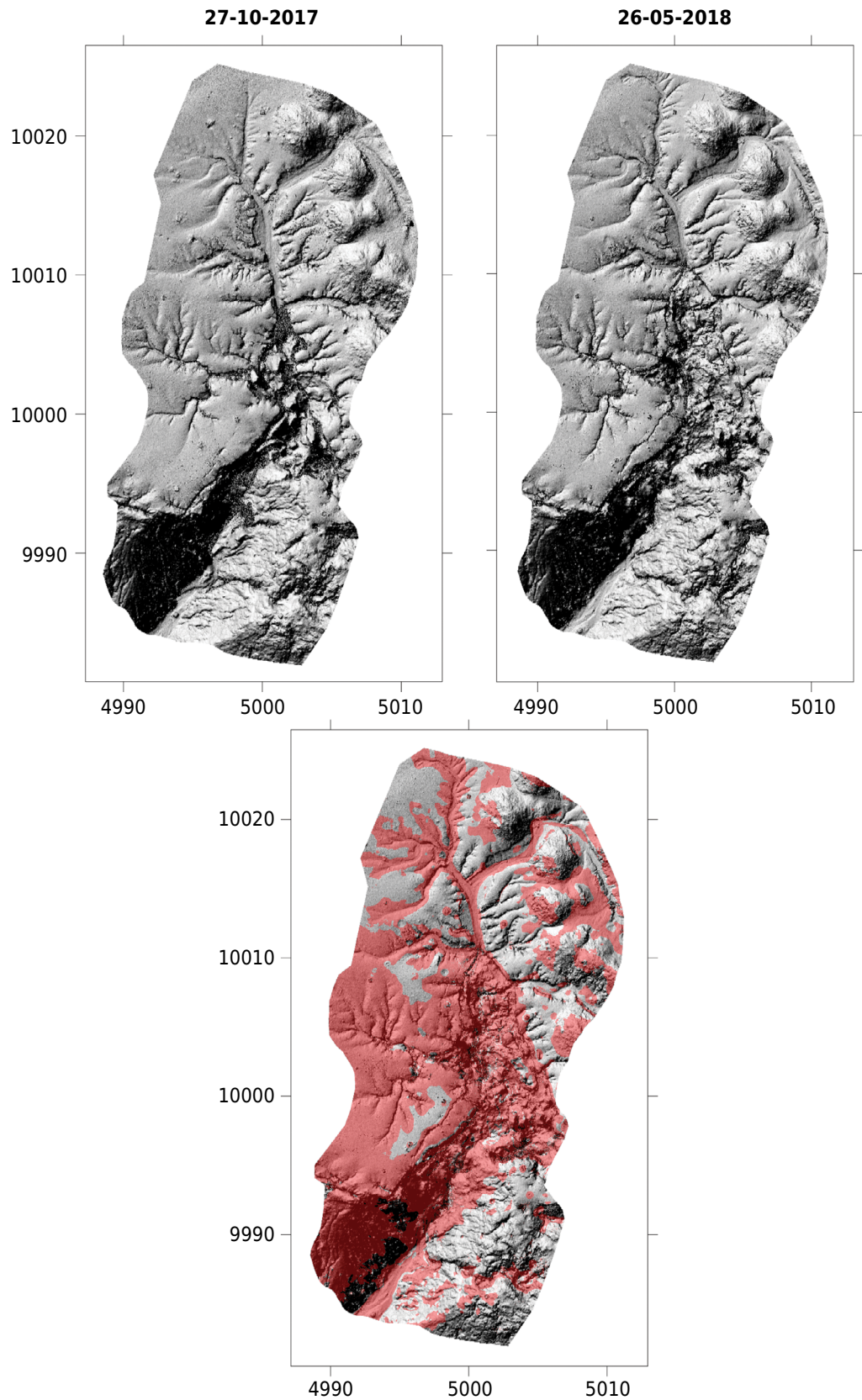
Figure 6. DEMs for the two surveys and the map showing the significant change, in red, over the studied period.

3 mm for *xyz*, as found in this study, are acceptable. These values are lower than those founded by Agüera-Vega et al. (2018), who also studied topography reconstruction in complex areas using UAV. A millimetric precision on this kind of survey is very important,

Table 3. The relative contribution of each erosion process in the gully system between October 2017 and May 2018

Erosion process	Sediments generation	Sediments stored	Sediments lost
	m³		
Sheet erosion	2.11	1.83	0.28
Rill erosion	5.69	0.76	4.93
Gully sidewall	63.39	14.38	49.01
Total	71.20	16.97	54.22
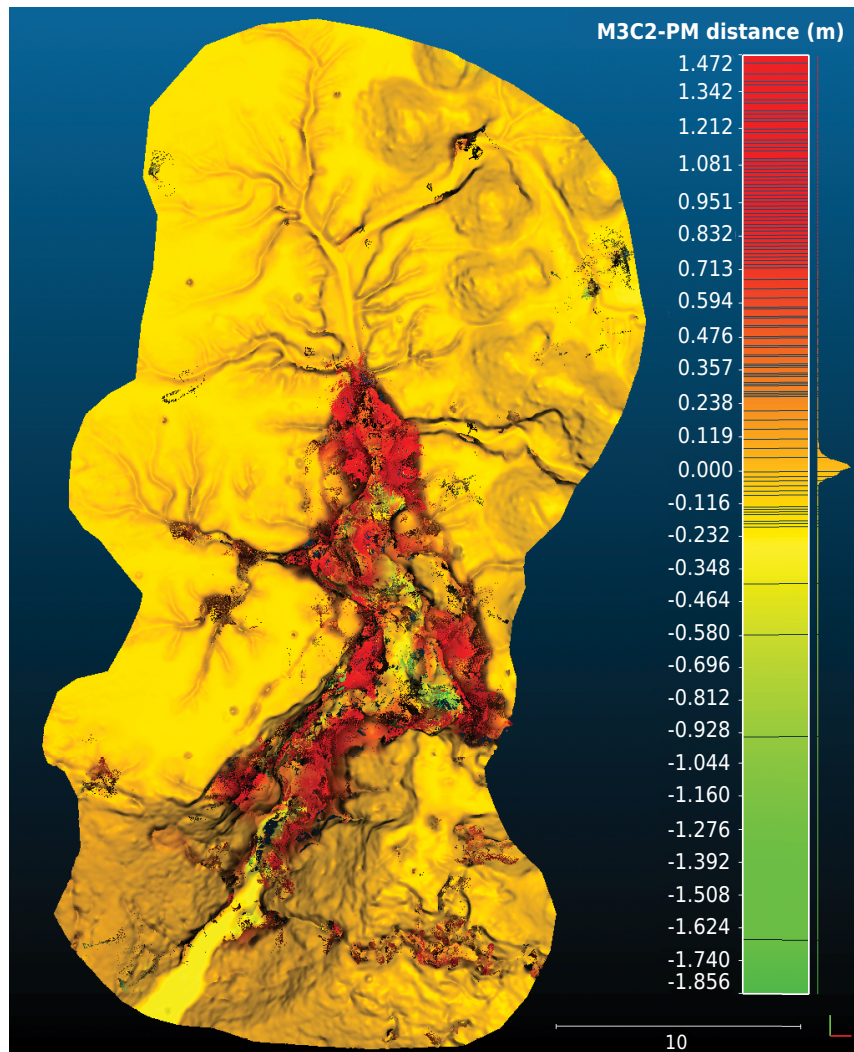
Figure 7. Point cloud showing the difference (M3C2-PM distance) between the October 2017 and May 2018 gully surveys. Colour intensity shows relative amounts of erosion (red) and deposition (green).

because it allows the assessment of all erosion types occurring in the area, from laminar erosion to large mass movements.

The largest photogrammetric errors, obtained in the regions of the most complex and shaded topography (Figure 4), can be reduced by performing flights on cloudy days with indirect light, increasing the number of oblique images and adding images taken in different height (Castillo et al., 2012; Gómez-Gutiérrez et al., 2014; Stöcker et al., 2015; Carbonneau and Dietrich, 2017; James et al., 2017b). Moreover, in areas where

there is large soil movement, such as the gully environment, it is advisable to use Real Time Kinematic Global Positioning System (RTK GPS) rather than total station (with an arbitrary local coordinate system) to collect GCP locations. This is to avoid repeatable GCP surveys due to the soil movements, especially in points located in the bed and near the gully sidewalls.

Source of sediments in the gully

The present study showed that the gully growth occurred towards the main erosion channels present in the area (Figures 6). The runoff concentrated in rills or depressions has the capacity to remove soil particles from the gully through sluicing (Lin et al., 2015). The gully side walls usually retreat due to three processes: mass displacement, the detachment of soil particles by splashes, or water running along gully banks (Chaplot et al., 2011). In the studied gully, the gully side wall retreated primarily due to the mass displacement, as showed by the M3C2-PM distance map (Figure 7). These results correspond to those of Vandekerckhove et al. (2003) and Hosseinalizadeh et al. (2019).

In contrast to previous gully erosion studies (Prosser and Slade, 1994; Inoubli et al., 2016; Ben Slimane et al., 2018), sediment generation in the studied gully was predominantly by the mass displacement process due to the erosion of the gully side walls. These results are similar to those found by De Rose et al. (1998) and Betts et al. (2003). Mass movements of gully side walls are also recognized by Harvey (2001) as an important process in the absence of extreme rainfall events and have been related to reactivation of gullies.

Studies indicate that in stabilized gullies it is expected that the amount of sediment stored in the channels will exceed the volume of soil lost in the gully system (Kasai et al., 2001; Betts et al., 2003). In the present study, 54.22 m^3 was lost from the gully system in only 8 months of monitoring, a value similar to that was found by Ben Slimane et al. (2018) for annual production of sediment in gullies. While just 16.97 m^3 of sediments generated were stored on the system.

These results showed that the studied gully is not stabilized yet. In that way, a detailed knowledge of the complex dynamics of gully evolution has implications for the correct management and application of stabilization practices of gully prone areas. The accelerated evolution of this gully demonstrates that conservation strategies should be applied in the early stages of the gully formation before the channels deepen and the mass movement processes accelerate the evolution of the gully erosion. Attempts to reduce the expansion of the gullies complex become less efficient in these advanced stages.

CONCLUSIONS

This study evaluated the relative contribution of the different erosive processes that occur simultaneously in a gully. The sediment sources of a gully were quantified remotely and with millimetric precision. Through the UAV photogrammetry, high resolution measurements were made, allowing to evaluate even the contribution of sheet erosion in the generation of sediment of the gully. This opens up new possibilities in the studies involving the dynamics of gullies, since the understanding of the spatial and temporal behaviour of the erosive processes are important in the development of control strategies and monitoring of the evolution of a gullies complex.

The results revealed that the main source of sediment in the gully studied was due to mass movement processes. Rills and laminar erosions contributed 8 and 3 %, respectively, to the total sediment yield, while mass movements corresponded with most of the sediment generation in the gully. Of the total sediment produced in the system, only 24 % was stored in the gully, indicating its high activity and instability.

ACKNOWLEDGEMENTS

AUTHOR CONTRIBUTIONS

Conceptualization: Ⓓ Bernardo Moreira Cândido (equal), Ⓓ Mike James (equal), Ⓓ John Quinton (equal), and Ⓓ Marx Leandro Naves Silva (equal).

Methodology: Ⓓ Mike James (lead) and Ⓓ Bernardo Moreira Cândido (supporting).

Software: Ⓓ Mike James (lead).

Validation: Ⓓ Bernardo Moreira Cândido (equal), Ⓓ Mike James (equal), and Ⓓ John Quinton (equal).

Formal analysis: Ⓓ Bernardo Moreira Cândido (lead) and Ⓓ Mike James (supporting).

Investigation: Ⓓ Bernardo Moreira Cândido (lead) and Ⓓ Wellington de Lima (supporting).

Resources: Ⓓ Marx Leandro Naves Silva (lead).

Data curation: Ⓓ Bernardo Moreira Cândido (lead), Ⓓ Mike James (supporting), and Ⓓ Wellington de Lima (supporting).

Writing – original draft: Ⓓ Bernardo Moreira Cândido (lead).

Writing – review and editing: Ⓓ Mike James (equal) and Ⓓ John Quinton (equal).

Visualization: Ⓓ Bernardo Moreira Cândido (lead).

Supervision: Ⓓ Mike James (equal), Ⓓ John Quinton (equal), and Ⓓ Marx Leandro Naves Silva (equal).

Project administration: Ⓓ Bernardo Moreira Cândido (equal), Ⓓ Mike James (equal), Ⓓ John Quinton (equal), and Ⓓ Marx Leandro Naves Silva (equal).

Funding acquisition: Ⓓ Marx Leandro Naves Silva (lead).

REFERENCES

Agüera-Vega F, Carvajal-Ramírez F, Martínez-Carricondo P, López JS-H, Mesas-Carrascosa FJ, García-Ferrer A, Pérez-Porras FJ. Reconstruction of extreme topography from UAV structure from motion photogrammetry. Measurement. 2018;121:127-38. https://doi.org/10.1016/j.measurement.2018.02.062

Allen PM, Arnold JG, Auguste L, White J, Dunbar J. Application of a simple headcut advance model for gullies. Earth Surf Proc Land. 2018;43:202-17. https://doi.org/10.1002/esp.4233

Bastola S, Dialynas YG, Bras RL, Noto LV, Istanbulluoglu E. The role of vegetation on gully erosion stabilization at a severely degraded landscape: a case study from Calhoun Experimental Critical Zone Observatory. Geomorphology. 2018;308:25-39. https://doi.org/10.1016/j.geomorph.2017.12.032

Ben Slimane A, Raclot D, Rebai H, Le Bissonnais Y, Planchon O, Bouksila F. Combining field monitoring and aerial imagery to evaluate the role of gully erosion in a Mediterranean catchment (Tunisia). Catena. 2018;170:73-83. https://doi.org/10.1016/j.catena.2018.05.044

Betts HD, Trustrum NA, De Rose RC. Geomorphic changes in a complex gully system measured from sequential digital elevation models, and implications for management. Earth Surf Proc Land. 2003;28:1043-58. https://doi.org/10.1002/esp.500

Blanco H, Lal R. Principles of soil conservation and management. Heidelberg: Springer; 2010.

Carbonneau PE, Dietrich JT. Cost-effective non-metric photogrammetry from consumer-grade sUAS: implications for direct georeferencing of structure from motion photogrammetry. Earth Surf Proc Land. 2017;42:473-86. https://doi.org/10.1002/esp.4012

Carollo FG, Di Stefano C, Ferro V, Pampalone V. Measuring rill erosion at plot scale by a drone-based technology. Hydrol Process. 2015;29:3802-11. https://doi.org/10.1002/hyp.10479

Casalí J, Loizu J, Campo MA, De Santisteban LM, Álvarez-Mozos J. Accuracy of methods for field assessment of rill and ephemeral gully erosion. Catena. 2006;67:128-38. https://doi.org/10.1016/j.catena.2006.03.005

Castillo C, Pérez R, James MR, Quinton JN, Taguas EV, Gómez JA. Comparing the accuracy of several field methods for measuring gully erosion. Soil Sci Soc Am J. 2012;76:1319-32. https://doi.org/10.2136/sssaj2011.0390

Chaplot V, Brown J, Dlamini P, Eustice T, Janeau JL, Jewitt G, Lorentz S, Martin L, Nontokozo-Mchunu C, Oakes E, Podwojewski P, Revil S, Rumpel C, Zondi N. Rainfall simulation to identify the storm-scale mechanisms of gully bank retreat. Agric Water Manage. 2011;98:1704-10. https://doi.org/10.1016/j.agwat.2010.05.016

Conoscenti C, Angileri S, Cappadonia C, Rotigliano E, Agnesi V, Maerker M. Gully erosion susceptibility assessment by means of GIS-based logistic regression: a case of Sicily (Italy). Geomorphology. 2014;204:399-411. https://doi.org/10.1016/j.geomorph.2013.08.021

Cook KL. An evaluation of the effectiveness of low-cost UAVs and structure from motion for geomorphic change detection. Geomorphology. 2017;278:195-208. https://doi.org/10.1016/j.geomorph.2016.11.009

De Rose RC, Gomez B, Marden M, Trustrum NA. Gully erosion in Mangatu Forest, New Zealand, estimated from digital elevation models. Earth Surf Proc Land. 1998;23:1045-53. https://doi.org/10.1002/(SICI)1096-9837(1998110)23:11<1045::AID-ESP920>3.0.CO;2-T

Desir G, Marín C. Factors controlling the erosion rates in a semi-arid zone (Bardenas Reales, NE Spain). Catena. 2007;71:31-40. https://doi.org/10.1016/j.catena.2006.10.004

Di Stefano C, Ferro V, Palmeri V, Pampalone V, Agnello F. Testing the use of an image-based technique to measure gully erosion at Sparacia experimental area. Hydrol Process. 2017;31:573-85. https://doi.org/10.1002/hyp.11048

d'Oleire-Oltmanns S, Marzolff I, Peter K, Ries J. Unmanned Aerial Vehicle (UAV) for monitoring soil erosion in Morocco. Remote Sens. 2012;4:3390-416. https://doi.org/10.3390/rs4113390

Easa SM. Estimating pit excavation volume using nonlinear ground profile. J Surv Eng. 1988;114:71-83. https://doi.org/10.1061/(ASCE)0733-9453(1988)114:2(71)

Ehiorobo JO, Audu HAP. Monitoring of gully erosion in an urban area using geoinformation technology. J Emerg Trends Eng Appl Sci. 2012;3:270-5.

Fonstad MA, Dietrich JT, Courville BC, Jensen JL, Carbonneau PE. Topographic structure from motion: a new development in photogrammetric measurement. Earth Surf Proc Land. 2013;38:421-30. https://doi.org/10.1002/esp.3366

Foster GR. Terraces and terracing. In: Hillel D, editor. Encyclopedia of soils in the environment. New York: Academic Press; 2005. p. 135-43.

Gómez-Gutiérrez Á, Schnabel S, De Sanjosé JJ, Contador FL. Exploring the relationships between gully erosion and hydrology in rangelands of SW Spain. Z Geomorphol. 2012;56:27-44. https://doi.org/10.1127/0372-8854/2012/S-00071

Gómez-Gutiérrez Á, Schnabel S, Berenguer-Sempere F, Lavado-Contador F, Rubio-Delgado J. Using 3D photo-reconstruction methods to estimate gully headcut erosion. Catena. 2014;120:91-101. https://doi.org/10.1016/j.catena.2014.04.004

Harvey AM. Coupling between hillslopes and channels in upland fluvial systems: implications for landscape sensitivity, illustrated from the Howgill Fells, northwest England. Catena. 2001;42:225-50. https://doi.org/10.1016/S0341-8162(00)00139-9

Harvey AM. Coupling between hillslope gully systems and stream channels in the Howgill Fells, northwest England: temporal implications. Géomorphologie. 1997;3:3-19. https://doi.org/10.3406/morfo.1997.897

Harvey AM. Process interactions, temporal scales and the development of hillslope gully systems: Howgill Fells, northwest England. Geomorphology. 1992;5:323-44. https://doi.org/10.1016/0169-555X(92)90012-D

Hosseinalizadeh M, Kariminejad N, Chen W, Pourghasemi HR, Alinejad M, Behbahani AM, Tiefenbacher JP. Spatial modelling of gully headcuts using UAV data and four best-first decision classifier ensembles (BFTree, Bag-BFTree, RS-BFTree, and RF-BFTree). Geomorphology. 2019;329:184-93. https://doi.org/10.1016/j.geomorph.2019.01.006

Inoubli N, Raclot D, Moussa R, Habaieb H, Le Bissonnais Y. Soil cracking effects on hydrological and erosive processes: a study case in Mediterranean cultivated vertisols. Hydrol Process. 2016;30:4154-67. https://doi.org/10.1002/hyp.10928

James MR, Robson S. Straightforward reconstruction of 3D surfaces and topography with a camera: Accuracy and geoscience application. J Geophys Res. 2012;117:F03017. https://doi.org/10.1029/2011JF002289

James MR, Robson S, d'Oleire-Oltmanns S, Niethammer U. Optimising UAV topographic surveys processed with structure-from-motion: Ground control quality, quantity and bundle adjustment. Geomorphology. 2017a;280:51-66. https://doi.org/10.1016/j.geomorph.2016.11.021

James MR, Robson S, Smith MW. 3-D uncertainty-based topographic change detection with structure-from-motion photogrammetry: precision maps for ground control and directly georeferenced surveys. Earth Surf Proc Land. 2017b;42:1769-88. https://doi.org/10.1002/esp.4125

Kaiser A, Neugirg F, Rock G, Müller C, Haas F, Ries J, Schmidt J. Small-scale surface reconstruction and volume calculation of soil erosion in complex Moroccan gully morphology using structure from motion. Remote Sens. 2014;6:7050-80. https://doi.org/10.3390/rs6087050

Kasai M, Marutani T, Reid LM, Trustrum NA. Estimation of temporally averaged sediment delivery ratio using aggradational terraces in headwater catchments of the Waipaoa River, North Island, New Zealand. Earth Surf Proc Land. 2001;26:1-16. https://doi.org/10.1002/1096-9837(200101)26:1<1::AID-ESP146>3.0.CO;2-9

Lague D, Brodu N, Leroux J. Accurate 3D comparison of complex topography with terrestrial laser scanner: application to the Rangitikei canyon (N-Z). ISPRS J Photogramm Remote Sens. 2013;82:10-26. https://doi.org/10.1016/j.isprsjprs.2013.04.009

Lin J, Huang Y, Wang M, Jiang F, Zhang X, Ge H. Assessing the sources of sediment transported in gully systems using a fingerprinting approach: an example from South-east China. Catena. 2015;129:9-17. https://doi.org/10.1016/j.catena.2015.02.012

Murtiyoso A, Grussenmeyer P, Börlin N, Vandermeerschen J, Freville T. Open source and independent methods for bundle adjustment assessment in close-range UAV photogrammetry. Drones. 2018;2:3. https://doi.org/10.3390/drones2010003

Poesen J. Challenges in gully erosion research. Landform Analysis. 2011;17:5-9.

Poesen J, Nachtergaele J, Verstraeten G, Valentin C. Gully erosion and environmental change: importance and research needs. Catena. 2003;50:91-133. https://doi.org/10.1016/S0341-8162(02)00143-1

Poesen J, Vandekerckhove L, Nachtergaele J, Oustwood Wijdenes D, Verstraeten G, van Wesemael B. Gully erosion in dryland environments. In: Bull LJ, Kirkby MJ, editors. Dryland rivers: hydrology and geomorphology of semi-arid channels. Hoboken: John Wiley & Son; 2002. p. 229-62.

Prosser IP, Slade CJ. Gully formation and the role of valley-floor vegetation, southeastern Australia. Geology. 1994;22:1127-30. https://doi.org/10.1130/0091-7613(1994)022<1127:GFATRO>2.3.CO;2

Sidorchuk A, Marker M, Moretti S, Rodolfi G. Gully erosion modelling and landscape response in the Mbuluzi River catchment of Swaziland. Catena. 2003;50:507-25. https://doi.org/10.1016/S0341-8162(02)00123-6

Siqueira Junior P, Silva MLN, Cândido BM, Avalos FAP, Batista PVG, Curi N, Lima W, Quinton JN. Assessing water erosion processes in degraded area using unmanned aerial vehicle imagery. Rev Bras Cienc Solo. 2019;43:e0190051. https://doi.org/10.1590/18069657rbcs20190051

Stöcker C, Eltner A, Karrasch P. Measuring gullies by synergetic application of UAV and close range photogrammetry - a case study from Andalusia, Spain. Catena. 2015;132:1-11. https://doi.org/10.1016/j.catena.2015.04.004

Valentin C, Poesen J, Li Y. Gully erosion: impacts, factors and control. Catena. 2005;63:132-53. https://doi.org/10.1016/j.catena.2005.06.001

Vandekerckhove L, Poesen J, Govers G. Medium-term gully headcut retreat rates in Southeast Spain determined from aerial photographs and ground measurements. Catena. 2003;50:329-52. https://doi.org/10.1016/S0341-8162(02)00132-7

Vandekerckhove L, Poesen J, Wijdenes DO, de Figueiredo T. Topographical thresholds for ephemeral gully initiation in intensively cultivated areas of the Mediterranean. Catena. 1998;33:271-92. https://doi.org/10.1016/S0341-8162(98)00068-X

Zabihi M, Pourghasemi HR, Motevalli A, Zakeri MA. Gully erosion modeling using GIS-based data mining techniques in Northern Iran: a comparison between boosted regression tree and multivariate adaptive regression spline. In: Pourghasemi H, Rossi M, editors. Natural Hazards GIS-based Spatial Modeling Using Data Mining Techniques. New York: Springer; 2019. p. 1-26.